Investigation into the bond strength of bitumen-fibre mastic

Abstract

The loss of bond strength in road pavement surfacing due to high traffic loads or moisture is a recurring problem, creating distresses such as ravelling, fatigue and rutting. It is, therefore, important to find a way to prevent or at least delay the loss of bond strength in asphalt mixtures. Such an improvement would lead to longer service life and a more comfortable drive for road users. This study describes how the pneumatic adhesion tensile testing instrument (PATTI) was used to examine the mechanism by which fibres influence the pull-off tensile strength of asphalt mastic. This study assesses the potential for chemical modification of the binder due to the presence of fibres, by means of work of cohesion and work of adhesion calculations, based on surface energy parameters and a binder drainage test. The study also evaluates the influence of different filler-bitumen ratios and fibre percentages on pull-off tensile strength. The test results indicate that the fibres enhance the pull-off tensile strength of the mastic, in addition to changing the failure mode from cohesive to hybrid, implying an improvement in the cohesive strength of the mastic.

1. Introduction

The bond strength is considered an important property affecting asphalt mixture performance. In an asphalt mixture, the aggregates are much stiffer and stronger than other components such as bituminous binder or mastic. Therefore, the possibility of failure is expected to be very small through the aggregates themselves, while there is a high possibility of failure in the material that bonds adjacent particles [1]. The loss of strength of cohesive bonds within the bitumen itself is termed cohesive failure, and adhesive failure is the breaking of the adhesive bonds between aggregate and bitumen or mastic materials, mainly due to the effect of water or low temperatures [2]. Under the effect of traffic loading forces, the aggregate particles tend to separate from each other. As these forces increase, failure occurs at the interfaces between the aggregate and mastic and/or inside the mastic film [3]. The loss of bond strength then compromises pavement integrity, and this could lead to different pavement failure types such as permanent deformation, ravelling and fatigue [4]. It is, therefore, important to investigate this phenomenon and find a way to prevent or at least reduce such deterioration in the bond strength.

The pull-off tensile strength test is commonly used to investigate the bond strength and failure type of a bitumen-aggregate mix. Past studies found that dry samples showed a cohesive failure, while moisture-conditioned samples showed a hybrid or adhesive failure [1, 5, 6]. The physicochemical properties of bitumen and aggregate surfaces, their surface energies, can be used to estimate the adhesive bond strength between the two [7]. Also, adding modification (polymer, acid, anti-stripping additive) to bitumen will influence the physicochemical properties and bond strength of bitumen [8].

Fibres have the potential to strengthen the bitumen phase, however studies have found that different types and amounts of fibre strengthen the modified asphalt in different ways [9, 10]. Past studies [11-13] have suggested that some fibres can absorb the light fraction of bitumen, in addition to the fact that adding fibres such as those of polyester, polyacrylonitrile, lignin and asbestos change the optimum bitumen content of an asphalt mixture. It is important to note that the mechanism of possible chemical modification of binder in contact with fibres remains in large part unknown. The binder drainage test can provide results that may help in understanding such modification.

This paper explores the influence of different types and percentages of fibre on the pull-off tensile strength of bituminous mastic. The effect of different filler-bitumen ratios on the pull-off tensile strength of fibre reinforced mastic is also investigated. To gain a better understanding of the chemical effect of fibre on the binding properties of bitumen, the work of cohesion and work of adhesion of drained binder, before and after mixing with fibres are calculated from surface energy components. The relationship between the work of cohesion and the pull-off tensile strength results of fibre reinforced mastic are investigated.

2. Materials and experimental methods

2.1 Materials

A combination of one penetration grade bitumen (40/60) [14], limestone filler with maximum size less than 0.063 mm and four fibre types (including two types of glass, cellulose and steel fibres recovered from tyres) were used. Table 1 lists the basic properties of these fibres. The glass fibres had two different lengths, 13 and 6 mm, classified as glass-l and glass-s respectively. Micrographs of these four fibre types and the fibre reinforced mastic are shown in Figures 1 to 3 using a Cryo-scanning electron microscope (Quanta 200 3D (FEI)). Samples were coated with platinum (Pt) at -160°C for 60 seconds at current of 10 mA. Accelerating voltage used was 10 kV for glass and cellulose and 15 kV for steel fibre. These show the needle-like structure of glass fibres; the spongy and flexible nature of cellulose; and the thick steel fibres coated with mastic.

2.2 Binder drainage test basket method

In this work, the basket method [15] was used to measure the binder drainage of fibre-reinforced mastic; 2.0% by volume of fibres in 80 g of binder. The resulting composite was placed into a steel mesh basket with sieve size 250 microns, which was then placed on a pre-wrapped tray in the oven at 160ºC for 3 hours. Binder flowed and drained through the mesh into the pre-wrapped tray. After 3 hours the steel mesh basket and pre-wrapped tray were removed from the oven and the mesh basket separated from the pre-wrapped tray. Once cooled the weight of the tray and drained binder was measured and the weight of drained material (D) calculated in percent.

2.3 Determination of asphaltene content

Asphaltene content in the drained binders was measured according to BS 2000 [16]. In this method the drained binder was mixed with heptane and heated under reflux, separating the binder into three components (asphaltenes, waxy substances and inorganic material). The remaining material was extracted by chromatographic separation.

2.4 Complex modulus test

A Bohlin Gemini 200 (DSR) was used in this study for measuring the rheological properties of base and drained binder. Eleven testing frequencies ranging from 0.1 to 10.0 (Hz) were used in the DSR tests with nine testing temperatures between 30 and 70ºC (at increments of 5ºC).

2.5 Pneumatic Adhesion Tensile Testing Instrument (PATTI) test

The Pneumatic Adhesion Tensile Testing Instrument (PATTI) is used to measure the cohesive and adhesive properties of a bitumen-aggregate system by measuring pull-off strength. The PATTI consists of a portable pneumatic adhesion tester, piston and reaction plate, air hose, camera and steel pull-out stub as shown in Figure 4. Aggregate substrates and pull-stubs have to be cleaned and dried at room temperature for at least 24 hours. Then, in order to remove any dust, the aggregate substrates and pull-stubs were wiped carefully using a damp paper towel. After that, all aggregate substrates and pull-stubs were placed in an oven at 80ºC for one hour. The fibre reinforced mastic was placed in an oven at 160ºC for 30 minutes, and by this time the mastic was fluid enough to coat the aggregate substrate. Then fibre reinforced mastic was poured onto the aggregate substrate, and a pull-stub was immediately pressed into it to achieve good mastic-aggregate adhesion [17]. Washers and three raised edges on the pull-stub are used to control the film thickness.

Samples were left for 24 hours at room temperature before testing in order to allow enough time for the aggregate and mastic to adhere and for the sample to reach the test temperature. After the mastic and substrate had cooled down the excess mastic at the edge of the pull-stub was carefully removed using a heated pallet knife. The test then consists of applying an upward pressure to the asphalt mastic by movement of the pull-out stub. Air pressure rate was fixed during the test in order to achieve repeatable results. The pull-off tensile strength of mastic indicates when the applied pressure exceeds the cohesive strength of the mastic or the adhesive bond strength between mastic and aggregate.

2.6 Surface energy measurement

Thermodynamic (adsorption) theory is widely accepted as an approach to explain the interfacial adhesion of a liquid-solid contact. This theory is based on the principle that an adhesive (the liquid) will adhere to a solid depending on the physical forces established at the interface, so long as contact is maintained. The interfacial forces are van der Waals and Lewis acid–base interactions. These forces are generally related to fundamental thermodynamic quantities, in particular the surface free energies of the materials involved [18]. The contact angles of binders and limestone aggregate were measured by using three selected probe liquids, distilled water, glycerol and diiodomethane [7].

3. Surface energy

According to past studies the cohesive and adhesive strengths of bitumen-aggregate systems have been successfully determined from the surface free energy ($\boldsymbol{\gamma}$) [19, 20]. Previous research investigated the technical criteria of test methods, such as accuracy, precision and the ability to provide all three surface energy parameters and recommended the Whilhelmy plate method (dynamic contact angle) for routine use [19]. Another study focused on evaluation of the resistance of asphalt mixtures to moisture damage, through understanding the mechanisms that influence the surface energy of aggregates and binders in addition to fracture behaviour of asphalt mixture. They found that the ratio of the adhesive bond energy under dry conditions to the adhesive bond energy under wet conditions is related to the asphalt mixture resistance to moisture damage [20]. The surface free energy is a measure of the amount of energy needed to form a unit area of new surface at the interface of the material [7].

The surface free energy ($\boldsymbol{\gamma}$) of a material comprises two components, a dispersive or Lifshitz-van der Waals component ($\boldsymbol{\gamma}^{LW}$) of electrodynamic origin, and a polar component ($\boldsymbol{\gamma}^{AB}$) caused by Lewis acid-base interactions [21] as shown in the following equation:

$$\boldsymbol{\gamma}^{\boldsymbol{total}} = \boldsymbol{\gamma}^{LW} + \boldsymbol{\gamma}^{AB} \qquad (1)$$

The acid-base components can be subdivided into a Lewis acid parameter of surface free energy ($\boldsymbol{\gamma}^{+}$) and a Lewis base parameter of surface free energy ($\boldsymbol{\gamma}^{-}$) as shown in the following equation:

$$\boldsymbol{\gamma}^{AB} = 2(\sqrt{\boldsymbol{\gamma}^{+}\boldsymbol{\gamma}^{-}}) \qquad (2)$$

By combining equations (1) and (2) the surface free energy (mJ/m^2) or (erg/cm^2) of a material can be defined as:

$$\gamma^{total} = \gamma^{LW} + 2(\sqrt{\gamma^{+}\gamma^{-}}) \quad (3)$$

3.1 Work of cohesion

The work of cohesion (W_C) can be defined as the energy required to separate the liquid or solid from itself and this depends on the attraction between molecules. The following equation describes the work of cohesion [8]:

$$W_C = 2\,\gamma^{total} \quad (4)$$

3.2 Work of adhesion

The work of adhesion (W_a) can be defined as the energy required to create new surfaces between two materials (solid-liquid); therefore, work of adhesion represents the amount of intermolecular interaction between two materials [22].

The work of adhesion is a dependent property of a solid-liquid pair. Accordingly the interfacial surface free energy of a material (binder or aggregate) is the combination of these non-polar (Lifshitz-van der Waals) and polar (Lewis acid/base) forces as shown in the following equation:

$$\gamma_{BA} = \gamma_{BA}^{LW} + \gamma_{BA}^{AB} \quad (5)$$

Where B and A represent bitumen and aggregate, respectively. The adhesive Lifshitz-van der Waals and Lewis acid/base bond strength can be determined by the following equations, respectively [23].

$$W^{LW} = \gamma_{B}^{LW} + \gamma_{A}^{LW} - \gamma_{BA}^{LW} \quad (6)$$

$$W^{AB} = \gamma_{B}^{AB} + \gamma_{A}^{AB} - \gamma_{BA}^{AB} \quad (7)$$

The Lifshitz-van der Waals solid-liquid surface energy is described by the following equations [23]:

$$\gamma_{BA}^{LW} = (\sqrt{\gamma_{B}^{LW}} - \sqrt{\gamma_{A}^{LW}})^2 \quad (8)$$

$$\gamma_{BA}^{AB} = 2(\sqrt{\gamma_B^+} - \sqrt{\gamma_A^+})(\sqrt{\gamma_B^-} - \sqrt{\gamma_A^-}) \quad (9)$$

By substituting these two equations (8) and (9) into equations (6) and (7) the following equation is obtained:

$$W_a = 2(\sqrt{\gamma_B^{LW}\gamma_A^{LW}} + \sqrt{\gamma_B^+\gamma_A^-} + \sqrt{\gamma_B^-\gamma_A^+}) \quad (10)$$

Where W^{LW} is the Lifshitz-van der Waals work of adhesion and W^{AB} is the Lewis acid/base work of cohesion.

In this paper the work of cohesion and work of adhesion, computed in this way, will be used to interpret the pull-off test data.

4. Results and analysis

4.1 Binder drainage test results

The results of the binder drainage tests are the average of three values as shown in Table 2. The results have low coefficient of variation, although higher for cellulose fibres due to having a similar level of variability and lower average drained binder percentage. The percentage of drained material reflects bitumen stability, which may be a function of the mechanical interaction of the fibres in the binder and absorption/adsorption of certain bitumen fractions by the fibres.

Cellulose fibre showed by far the highest stabilisation and absorption/adsorption effect compared to the other fibre types, as expected due to the surface texture and large surface area of cellulose fibre (see Table 1), giving high absorption and retention of liquid media. Other fibre types (glass and steel) held lower amounts of bitumen. These results may reflect the amount of bitumen adhering to the fibre surfaces. Samples of base binder and drained binders were taken for analysis of asphaltene content and surface energy components.

4.2 Asphaltene test results

Asphaltenes are the bitumen fraction that is insoluble in low molecular weight paraffin, such as propane, n-butane, n-pentane, n-heptane and n-hexane [24]. They are relatively high in heteroatoms such as nitrogen, oxygen, carbon and hydrogen with sulphur. Asphaltenes are the largest fraction of bitumen, responsible for the increase in thickening, strength and stiffness of the bitumen and non-Newtonian rheological behaviour [24]. This paper measured the influence of different fibre types on the asphaltene content of base binder to explore the effect on bitumen chemistry of adding fibres. A previous study indicated that high asphaltene content might have led to increased cohesive and adhesive strength of base binder [25].

Two tests were performed for each fibre type, and the average asphaltene content is reported in Table 3. The drained binders showed higher asphaltene content compared to the base binder. As noted in the introduction, previous studies showed that fibres can adsorb /absorb the light fraction of bitumen [11-13], and it is important to note that the cellulose fibres retained over 50% of the bitumen in the drainage test while the other fibres retained about 25%, compared to 3% for the sample without fibres. Preferential adhesion of the lighter binder fraction would lead to higher asphaltene content in the drained binder. Also, steel fibre, as a thermal conductor, may influence the bitumen heating process and lead to more ageing of the bitumen during the draining process and hence, lead to higher asphaltene content. The results suggest that the presence of fibres leads to higher asphaltene content, however, due to the variability in the asphaltene test results, it is hard to draw conclusions about any differences. For this reason the rheological properties of the drained binders were evaluated by creating complex modulus master curves.

4.3 Complex modulus master curve of base and drained binder

Figure 5 shows the complex modulus master curves for base binder, drained base binder and drained binder after mixing with fibres. A considerable difference in the complex modulus values of drained binder after mixing with fibres, compared to both base and drained base binder can be seen. This increase in complex modulus could be due to the fibre affecting the chemical composition of the binder by adsorption/absorption of different fractions, mainly lighter fractions. A previous study, using chromatography, indicated that the fibre could influence the absorption of different fractions, particularly lighter fractions [26]. This result reflects the asphaltene content results, as the asphaltene content increased for drained binder after mixing with fibres, as shown in Table 3.

It is important to note that the complex modulus values of drained binder after mixing with glass and steel fibre were almost the same. Cellulose fibre showed higher complex modulus compared to other fibre types. This increase in complex modulus may be because cellulose fibre had lower drained binder percentage (Table 2), indicating retention of more of the bitumen.

4.4 Pneumatic adhesion tensile testing instrument (PATTI)

The PATTI test was used to measure the influence of fibres on mastic bond strength. Three filler-bitumen ratios (0.8, 1.0 and 1.2) and three fibre contents (0.5, 1.0 and 2.0% by bitumen volume) were used in this investigation. Failure strength results are shown in Figures 6 to 8 and the mode of failure in Table 4, as illustrated in Figures 9 and 10.

4.4.1 Influence of fibre content and type

Three tests were performed for each mastic type, and the average tensile strength was reported, as shown in Figures 6 to 8, where error bars represent plus and minus one standard error (standard deviation divided by the square root of number of samples). The tensile strengths of different fibre types and filler-bitumen ratios were reasonably repeatable, indicating that the application of a constant rate of air pressure was successful for these tests. The specimens exhibited a linear response to the increase in pressure until the pressure overcame the cohesive strength of the mastic or the adhesive strength of the mastic-aggregate interface and then rapidly decreased to zero.

It can be seen that on average, all fibre types increased the pull-off tensile strength compared to the base mastic. Table 5 gives the average results along with t-test results, comparing fibre mastics to the base binder, for the three filler-bitumen ratios. Most fibre percentages and types show statistically significant increases in the pull-off strength.

The glass-l fibre showed the highest increase in bond strength among all fibre types. This increase may be due to two reasons. Firstly, glass fibre contains silicon dioxide (SiO_2) and aluminium oxide (Al_2O_3). This chemical combination can form strong chemical bonds with sulfoxides and carboxylic acids in bitumen [27, 28]. Secondly, glass fibre dimensions (length and width) may help the fibres to cross over each other to form three dimensional networks. These networks then provide support to the composite structure by holding the components together and spreading stresses [29].

Base mastics with different filler-bitumen ratios showed cohesive failure (failure within the mastic). The failure type changed from cohesive to hybrid (partly adhesive failure between aggregate and mastic) with an increase in the pull-off strength when 1.0 and 2.0% cellulose and glass-s fibres were used as a modification for 1.0 and 1.2 filler-bitumen ratios. This implies an improvement in the cohesive strength of the mastic with the increase in fibre content, as shown in Figures 7 and 8. This behaviour may be explained by the higher fibre content both mechanically stabilizing the material and/or absorbing/adsorbing the bituminous binder (see Table 2) [30]. The latter is likely with cellulose fibre since the surface texture of cellulose fibres comprises many interweaved branches with non-uniform sizes and rough surfaces, which will increase the specific surface area and hence the absorption/adsorption capability (see Table 1), as shown in SEM images (see Figure 2). These features of cellulose fibre might explain the hybrid failure at 0.8 filler-bitumen ratio for mastic modified by cellulose fibre, whereas other fibre types exhibited a cohesive failure, as shown in Table 4 and Figure 9 a.

On the other hand, the longer steel and glass-l fibre samples showed a hybrid failure for all fibre percentages at 1.0 and 1.2 filler-bitumen ratios. This could be due to the dimensions of these fibres, leading to a more effective network and therefore enhanced reinforcement effects.

4.4.2 Influence of filler-bitumen ratio

The results (Figures 6, 7 and 8) showed that the pull-off tensile strength increased with the increase in the filler-bitumen ratio. A possible explanation for this might be that adding more filler enhanced the interaction between the bitumen and the filler particles [31]. Bituminous binders are non-polar, while molecules of limestone are more polar. This may help to satisfy the energy demand of the aggregate surface by improving the adhesion between the aggregate and the mastic [28, 32].

There is a decrease in the pull-off tensile strength of the 1.2 filler-bitumen ratios at 2.0% fibre content, particularly for cellulose, glass-l and steel fibres. This may indicate that adding more fibre with a high absorption/adsorption and/or large surface area led to an increase in the percentage of voids in the matrix [33, 34]. The stress applied to the specimen may have been concentrated around these voids, and the fracture may have begun at these points. Moreover, as the percentage of filler and fibre increased, the composite became stiffer and was, therefore, more likely to show brittle behaviour. This suggests that when adding more fibre and filler, there should be enough binder in the mix to reduce the voids in the mastic.

It is important to note that the modulus and Poisson's ratio of steel and glass fibres are very large compared to the matrix, and therefore a concentration of stress will occur at the interface. Also, steel fibre has large thickness and according to previous studies, the stress concentration area depends on the fibre thickness and this area will increase as fibre thickness increases [35] (see Figure 11).

4.5 Surface energy

The dynamic contact angle (DCA) measurement of bitumen was used in this study. The contact angles were measured for each drained binder for each probe liquid, and the contact angle was taken as the average of four or five replicates and the variation between results was low, as shown in Table 6. The results for the surface energy components of the drained binders are shown in Table 7 in which γ_s^{AB} represents the polar surface energy component of the solid and γ_s^{LW} represents the non-polar (Lifshitz-van der Waals) surface energy component of the solid. The results for the surface energy components of the drained binders showed more variation in the γ_s^{AB} values than the γ_s^{LW} values, ranging from 0.19 to 1.78 mJ/m^2, as shown in Table 7. The results showed that the bituminous binder molecular constituent forces are mainly Lifshitz-van der Waals (non-polar) in character [36].

The surface energy components of limestone aggregate were determined by using a dynamic vapour sorption (DVS) approach, and the results are shown in Table 8. This method is usually used for high surface energy materials such as aggregate, and the advantage of this method is that it takes into consideration the irregular shape and surface texture of the aggregate [7]. The surface energy of limestone aggregate was found to be 104.19 mJ/m^2.

4.6 Work of cohesion and adhesion

The results for work of cohesion ($2\gamma^{total}$) of the base drained binder and drained binder after mixing with fibres are shown in Table 9. Table 4 shows the mode of failure in the PATTI tests and reveals that the 0.8 filler-bitumen ratio mastics consistently failed by fully cohesive failure. It is, therefore, interesting to compare the pull-off strength for these mastics to the work of cohesion of the binders. The pull-off strengths are included in Table 9 and Figure 12 shows a comparison between work of cohesion and pull-off tensile strength. The work of cohesion results cover just a small range of values but it was found that higher pull-off tensile strength corresponds to higher work of cohesion. These results are consistent with data obtained in another recent study [8].

One consistent finding in this study is that all drained binders after mixing with fibres, showed higher values for work of cohesion compared to that of the drained base binder. Also, it is noted that all unmodified mastics showed a cohesive failure, while highly modified mastics showed a hybrid failure (partially between aggregate and bitumen) together with an increase in pull-off strength. These observations indicate that adding fibre increases the cohesive strength of the mastic leading to hybrid failure.

The work of adhesion results are shown in Table 10. It is interesting to note that drained binder after mixing with cellulose fibre had the lowest value of work of adhesion. This is due to the low value of the Lewis base parameter of surface free energy of the drained binder after mixing with cellulose fibre. This finding may explain the hybrid failure for mastic modified with cellulose fibre at 0.8 filler-bitumen ratio and 1.0 and 2.0% fibre, while other modified mastics showed cohesive failure at this filler-bitumen ratio (see Table 4). These surface energy results support the ability of the (PATTI) test to detect differences in bond strength. However, none of the pull-off tensile strength samples showed adhesive failure because pull-off tensile strength tests were done at room temperature (20°C) and in dry conditions. These conditions eliminate the possibility of adhesive failure. Therefore, this study was not able to find a relationship between the pull-off tensile strength and the work of adhesion.

4.7 Conclusions

This paper has examined the influence of fibres on bitumen mastic, based on pull-off tensile strength, asphaltene content, surface energy measurement and scanning electronic microscopy. The following conclusions are offered:

- Fibre asphalt mastics were observed using a scanning electron microscope (SEM). The formation of three-dimensional networks was observed for glass and steel fibre reinforced mastic.
- The drainage test results showed that cellulose fibre can retain more than 55% of binder. Other fibre types (glass and steel) can retain up to 30% of binder.
- All fibre types increased the asphaltene content and complex modulus of the drained binder compared to the base binder. However, the differences between asphaltene contents for different fibre types were too small to discriminate between them with confidence.
- Adding fibre led to an increased pull-off tensile strength of the mastics, at the same time changing the failure mode from cohesive to hybrid, implying an improvement in cohesive strength of the mastic.
- There was a general reduction in the pull-off tensile strength of the 1.2 filler bitumen ratio at high fibre content (2.0%).
- The surface energy of drained binder after mixing with fibres was estimated by dynamic contact angle (DCA) measurements. The contact angle results for each

drained binder varied within a narrow range, making this a useful test for characterising these materials.

- In general, there is a good agreement between work of the cohesion and pull-off tensile strength for 0.8 filler bitumen ratio and higher work of cohesion results in higher pull-off tensile strength where the mode of failure is cohesive.

List of tables

Table 1 Basic properties of fibres

Fibre type	Specific density (g/cm³)	Length (µm)	Width (µm)	Modulus of elasticity at 23 °C (GPa)	Specific surface area (m²/g)
Cellulose	1.50	20 to 2,500	25	-	138.53
Glass-s	2.58	6,000	12 to 20	80.3	8.85
Glass-l	2.58	13,000	12 to 20	80.3	14.36
Steel	7.85	4,000 to 12,000	180 to 300	210*	-

*Standard steel fibre modulus

Table 2 Results of binder drainage test (basket method)

Fibre type	Percent of drained material (average of three results) (%)	Coefficient of variation (%)	Standard error
Base binder	97.0	0.7	0.41
Cellulose	43.4	3.0	0.74
Glass-s	74.9	2.2	0.96
Glass-l	71.1	2.4	0.97
Steel	72.1	1.2	0.49

Table 3 Asphaltene content test results

Binder type	Asphaltene content (%)	Coefficient of variation (%)	Standard error
Base binder	12.7	1.1	0.10
Drained base binder	14.7	0.5	0.05
Drained cellulose	15.9	3.3	0.26
Drained glass-s	14.9	4.0	0.57
Drained glass-l	15.7	5.1	0.46
Drained steel	15.5	5.0	0.55

Table 4 Failure mode in fibre modified asphalt mastic

Mastic type	**f/b***	**Failure type**			
		0.0% vol.	0.5% vol.	1.0% vol.	2.0% vol.
Base mastic	0.8	Cohesion	-	-	-
	1.0	Cohesion	-	-	-
	1.2	Cohesion	-	-	-
Cellulose fibre mastic	0.8	-	Cohesion	Hybrid	Hybrid
	1.0	-	Cohesion	Hybrid	Hybrid
	1.2	-	Cohesion	Hybrid	Hybrid
Glass-s fibre mastic	0.8	-	Cohesion	Cohesion	Cohesion
	1.0	-	Cohesion	Hybrid	Hybrid
	1.2	-	Cohesion	Hybrid	Hybrid
Glass-l fibre mastic	0.8	-	Cohesion	Cohesion	Cohesion
	1.0	-	Hybrid	Hybrid	Hybrid
	1.2	-	Hybrid	Hybrid	Hybrid
Steel fibre mastic	0.8	-	Cohesion	Cohesion	Cohesion
	1.0	-	Hybrid	Hybrid	Hybrid
	1.2	-	Hybrid	Hybrid	Cohesion

*f/b: filler-bitumen ratio

Table 5 Pull-off tensile strength t-test results

f/b ratio*	Fibre	Mean (MPa)	t-stat	p-value	Significant**
0.8	Base mortar	1.19	-	-	-
	0.5% Glass-s	1.61	4.828	0.0202	Yes
	0.5% Glass-l	1.71	5.677	0.0054	Yes
	0.5% Cellulose	1.56	4.121	0.0271	Yes
	0.5% Steel	1.44	2.731	0.0359	Yes
	1% Glass-s	1.76	4.139	0.0072	Yes
	1% Glass-l	1.78	6.394	0.0038	Yes
	1% Cellulose	1.64	4.703	0.0091	Yes
	1% Steel	1.76	4.117	0.0073	Yes
	2% Glass-s	1.85	6.403	0.0038	Yes
	2% Glass-l	1.95	8.388	0.0069	Yes
	2% Cellulose	1.84	6.348	0.0039	Yes
	2% Steel	1.81	6.275	0.0041	Yes
1.0	Base mortar	1.25	-	-	-
	0.5% Glass-s	1.61	3.775	0.0317	Yes
	0.5% Glass-l	1.78	3.350	0.0393	Yes
	0.5% Cellulose	1.69	4.525	0.0101	Yes
	0.5% Steel	1.55	3.641	0.0339	Yes
	1% Glass-s	1.78	3.798	0.0160	Yes
	1% Glass-l	2.06	5.222	0.0068	Yes
	1% Cellulose	1.76	6.398	0.0038	Yes
	1% Steel	1.88	5.446	0.0060	Yes
	2% Glass-s	2.10	8.518	0.0017	Yes
	2% Glass-l	2.16	8.794	0.0015	Yes
	2% Cellulose	2.09	11.947	0.0034	Yes
	2% Steel	1904	10.204	0.0047	Yes
1.2	Base mortar	1.72	-	-	-
	0.5% Glass-s	1.93	2.174	0.0808	No
	0.5% Glass-l	2.08	4.087	0.0274	Yes
	0.5% Cellulose	1.99	3.410	0.0907	No
	0.5% Steel	2.00	2.617	0.0601	No
	1% Glass-s	2.03	2.372	0.0705	No
	1% Glass-l	2.47	7.338	0.0090	Yes
	1% Cellulose	2.10	3.353	0.0219	Yes
	1% Steel	2.12	3.242	0.0238	Yes
	2% Glass-s	2.06	2.368	0.0493	Yes
	2% Glass-l	2.17	4.786	0.0204	Yes
	2% Cellulose	2.06	4.316	0.0724	No
	2% Steel	2.05	3.405	0.0764	No

*f/b: filler-bitumen ratio.
** indicates significant at the 95 percent confidence interval.

Table 5 Contact angle measurement of bitumen binder

	Contact Angle in Diiodomethane		Contact Angle in Glycerol		Contact angle in Water	
Sample	Average (°)	CV* (%)	Average (°)	CV (%)	Average (°)	CV (%)
Drained base binder	82.99	1.05	92.12	1.18	101.54	0.52
Drained cellulose	80.23	1.32	92.56	0.08	101.58	1.36
Drained glass-s	78.22	2.69	94.26	1.08	95.32	1.19
Drained glass-l	75.99	1.36	94.96	0.33	98.09	0.67
Drained steel	79.58	2.28	95.23	0.45	97.25	0.54

*CV: coefficient of variation

Table 6 Surface energy components of drained binder

Binder type	γ_s^{LW}	$\gamma_s^{AB} = 2\sqrt{\gamma^+\gamma^-}$	$\gamma^{\,total}$ *(mJ/m²)*
Drained base binder	15.99	1.78	17.77
Drained cellulose	17.38	1.30	18.68
Drained glass-s	18.41	0.46	18.88
Drained glass-l	19.59	0.59	20.18
Drained steel	17.71	0.19	17.90

Table 7 Surface energy components of limestone aggregate

Aggregate	γ_s^{LW}	$\gamma_s^{AB} = 2\sqrt{\gamma^+\gamma^-}$	$\gamma^{\,total}$ (mJ/m²)
Limestone	65.81	38.38	104.19

Table 8 Work of cohesion (2 γ^{total}) and pull-off tensile strength values (0.8 filler-bitumen ratio)

Sample	Pull-off tensile strength (MPa) 0.8 f/b ratio	Work of cohesion (mJ/m²)
Drained base binder	1.19	35.53
Drained cellulose	1.84	37.35
Drained glass-s	1.85	37.76
Drained glass-l	1.95	40.36
Drained steel	1.81	35.80

Table 9 Work of adhesion results

Sample	Work of adhesion (mJ/m²)
Drained base binder	122.69
Drained cellulose	125.18
Drained glass-s	172.88
Drained glass-l	158.64
Drained steel	163.21

List of figures

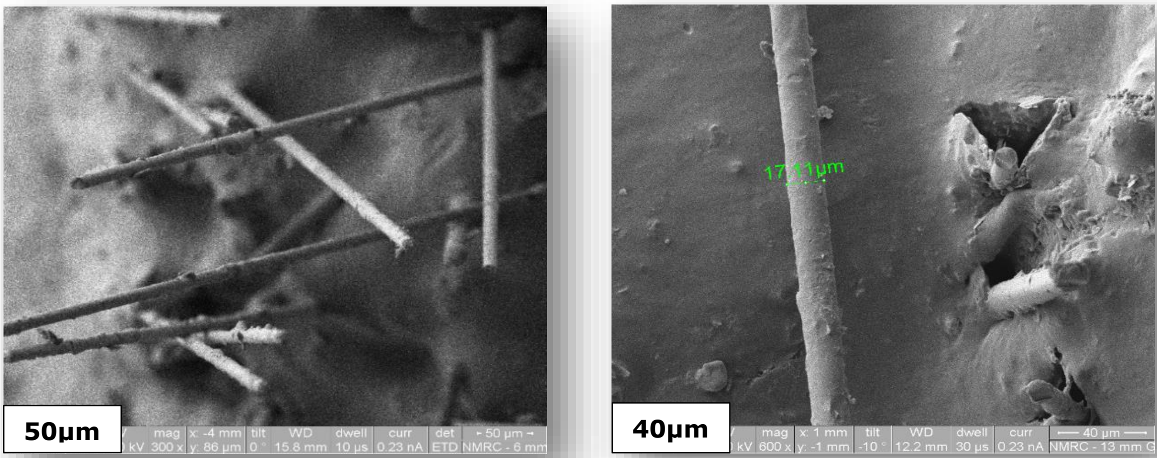

Figure 1 SEM images of glass fibre modified asphalt mastics

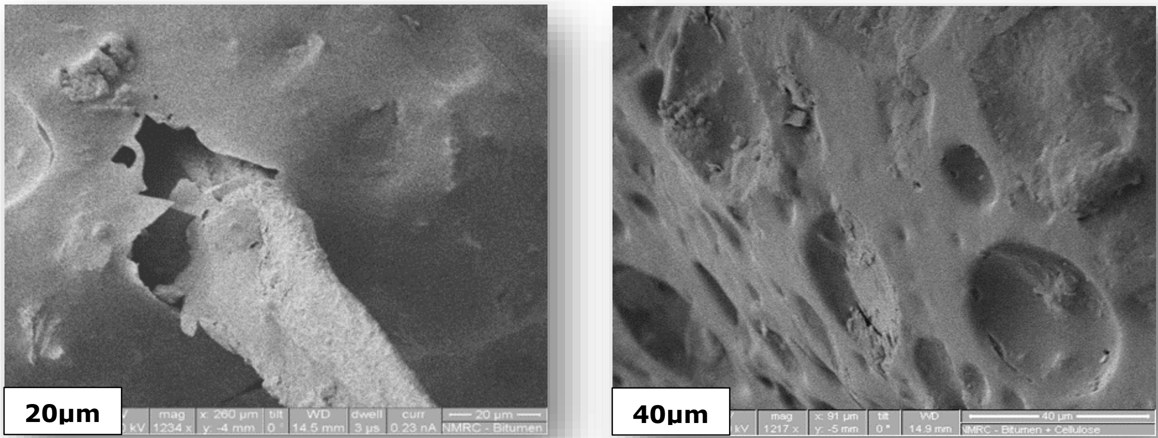

Figure 2 SEM images of cellulose fibre modified asphalt mastics

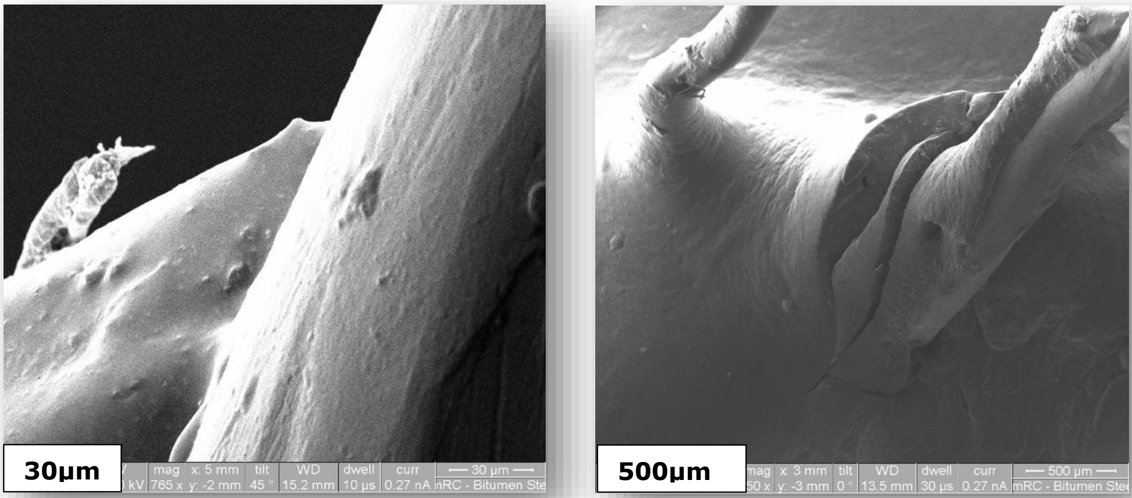

Figure 3 SEM images of steel fibre modified asphalt mastics

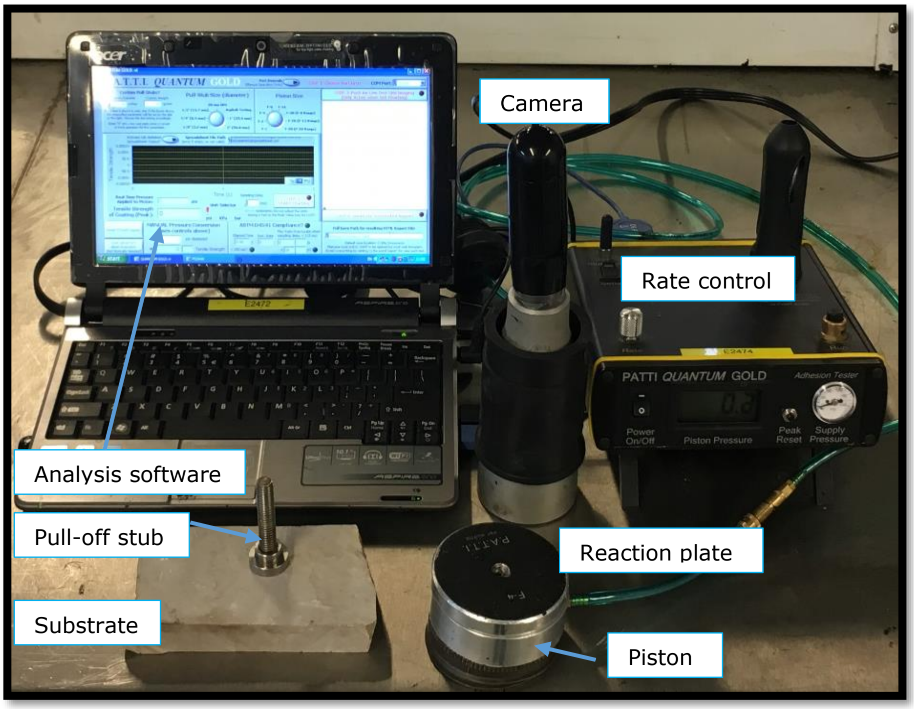

Figure 4 General representation of PATTI test [17]

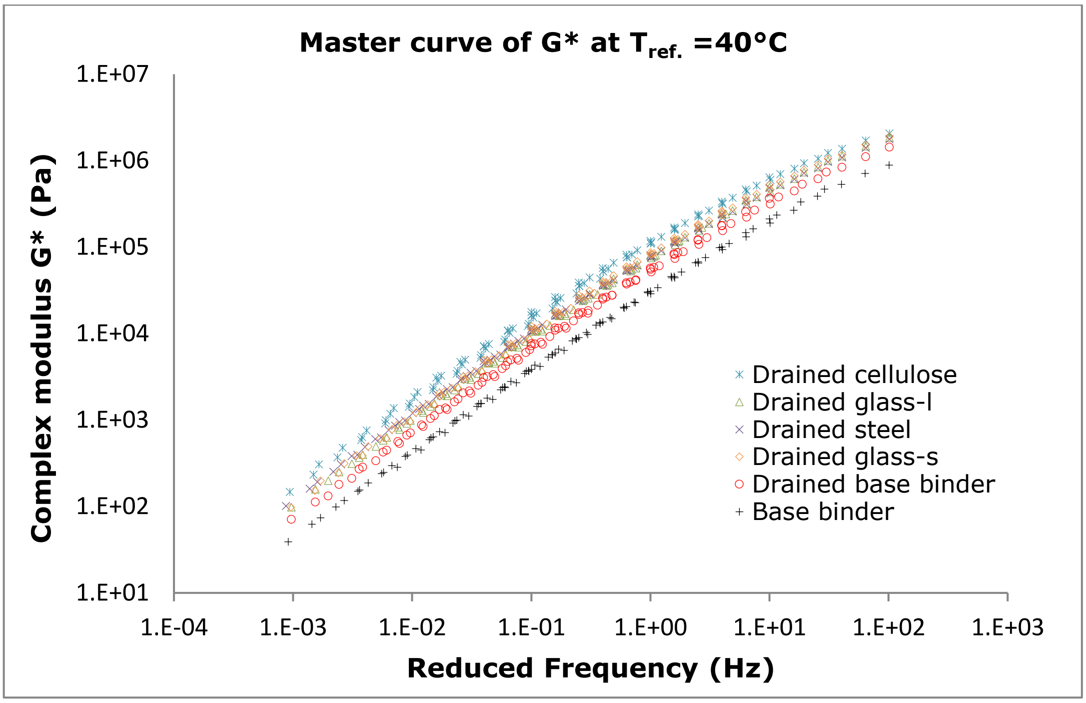

Figure 5 Complex modulus master curves for drained binders (2.0% fibre by volume)

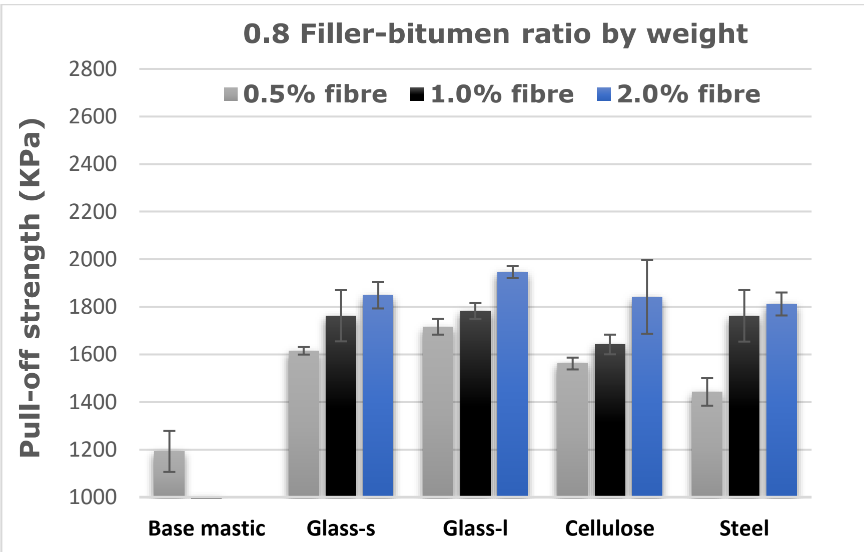

Figure 6 Pull-off tensile strength of base and modified mastics

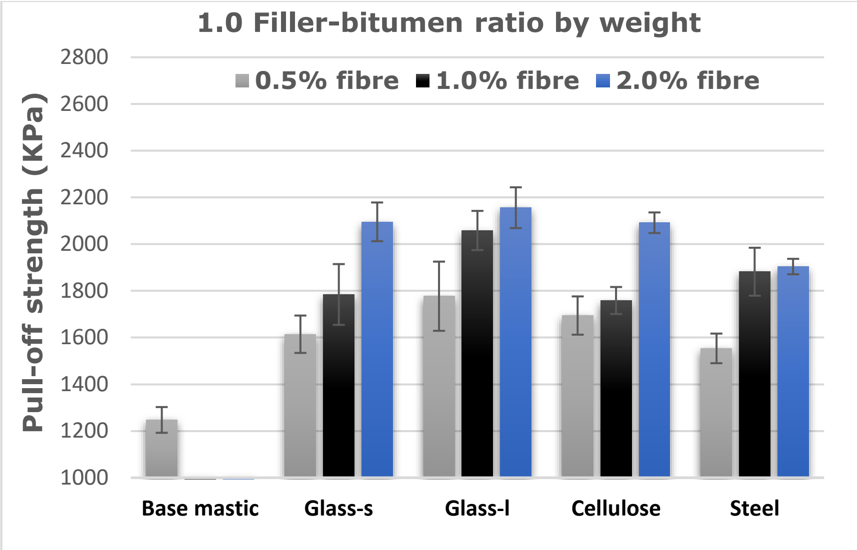

Figure 7 Pull-off tensile strength of base and modified mastics

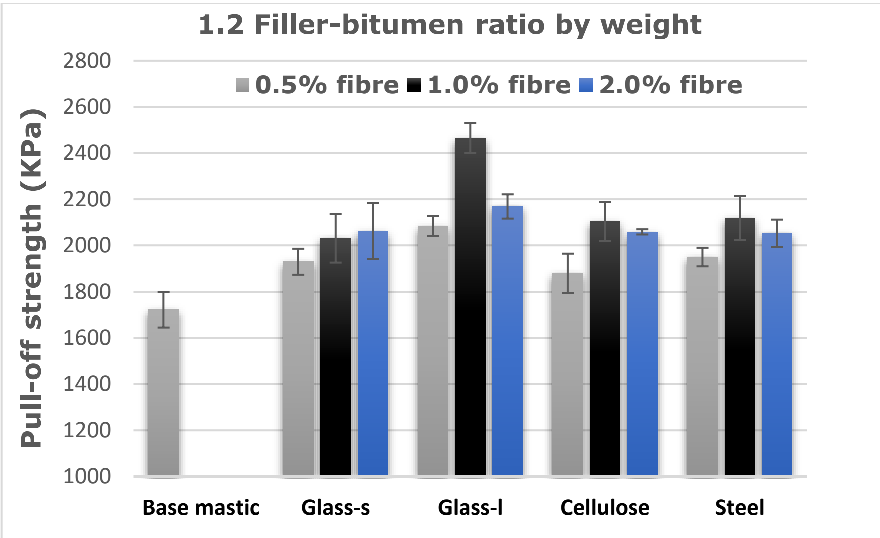

Figure 8 Pull-off tensile strength of base and modified mastics

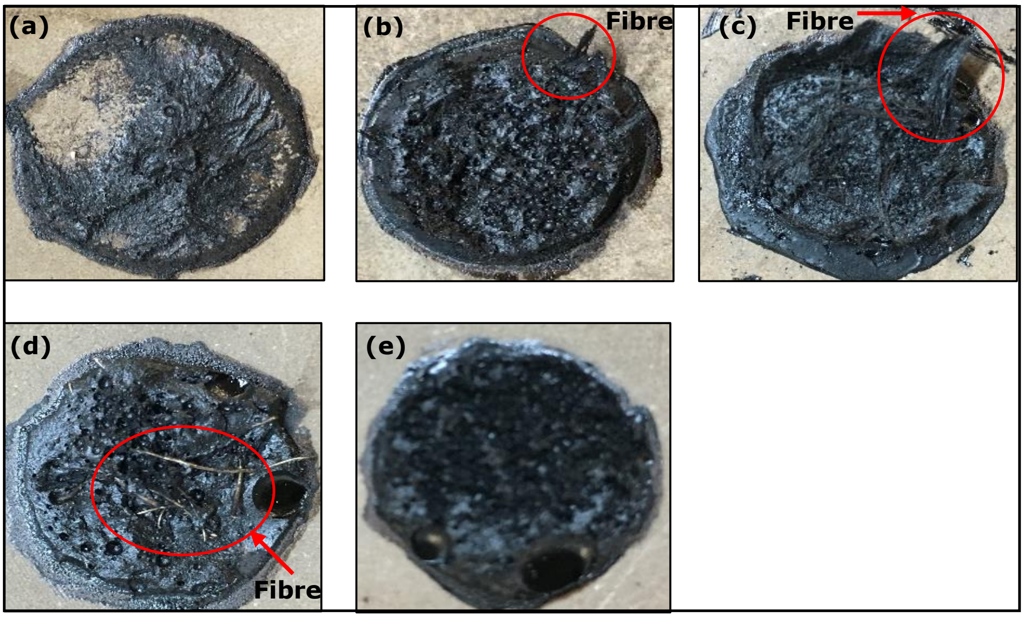

Figure 9 Failure surfaces of 0.8 filler bitumen ratio asphalt mastic with limestone aggregate with different fibre types: (a) cellulose, (b) glass-s, (c) glass-l, (d) steel and (e) base mastic.

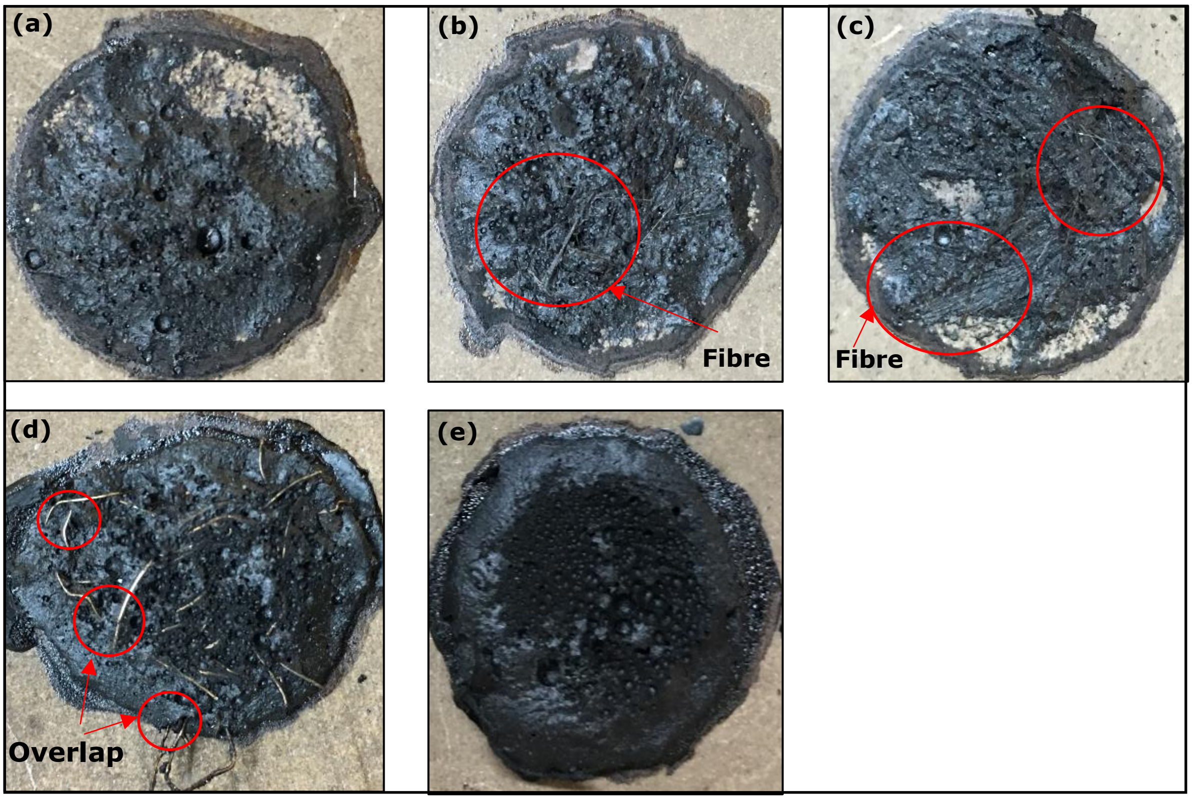

Figure 10 Failure surfaces of 1.2 filler bitumen ratio asphalt mastic with limestone aggregate with different fibre types: (a) cellulose, (b) glass-s, (c) glass-l, (d) steel and (e) base mastic.

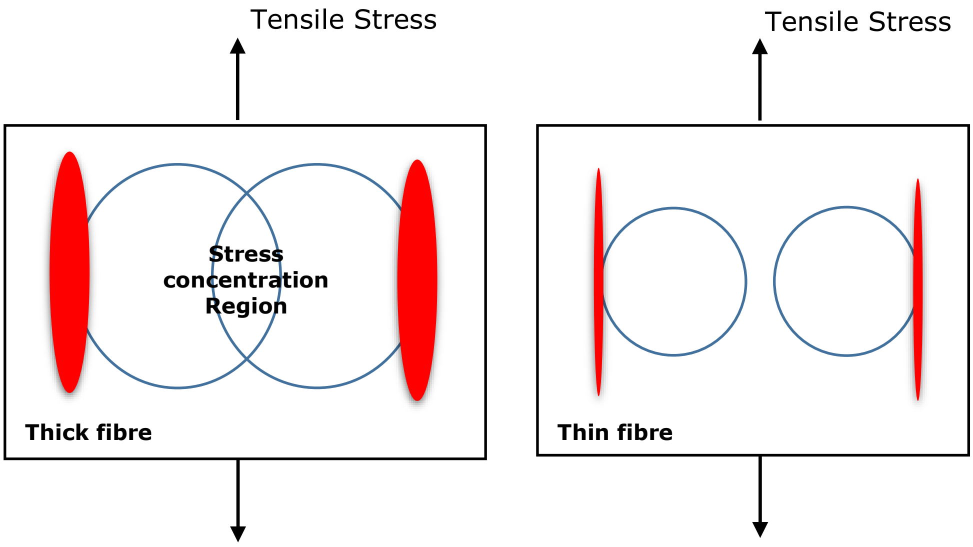

Figure 11 Stress concentration due to fibre size [35]

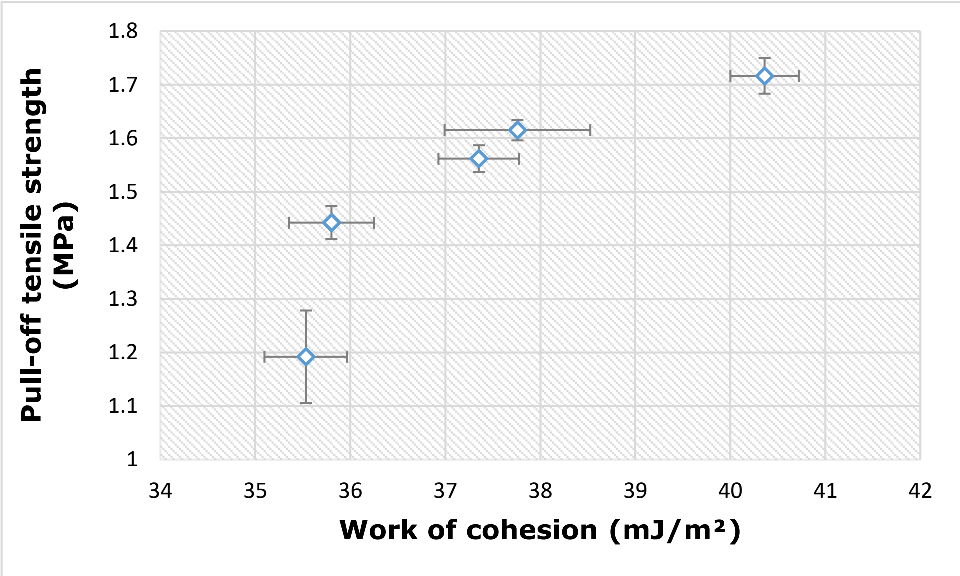

Figure 12 Comparison between work of cohesion of drained binders and pull-off tensile strength of 0.8 filler-bitumen ratio mastics (specimens undergoing cohesive failure)

Acknowledgment

The authors would like to acknowledge the financial support from the Higher Committee for Education Development in Iraq. The authors acknowledge the support provided by the Nottingham Transportation Engineering Centre (NTEC) at the University of Nottingham, United Kingdom. The authors thank the Nanoscale and Microscale Research Centre (nmRC) at the University of Nottingham, United Kingdom for providing access to instrumentation and Dr Christopher D. J. Parmenter for technical assistance.

References

[1] L. Mo, Damage development in the adhesive zone and mortar of porous asphalt concrete, TU Delft, Delft University of Technology, 2010.

[2] S. Caro, E. Masad, A. Bhasin, D. Little, Coupled micromechanical model of moisture-induced damage in asphalt mixtures, Journal of Materials in Civil Engineering 22(4) (2009) 380-388.

[3] M.I. Hossain, R.A. Tarefder, Behavior of asphalt mastic films under laboratory controlled humidity conditions, Construction and Building Materials 78 (2015) 8-17.

[4] D.-W. Cho, K. Kim, The mechanisms of moisture damage in asphalt pavement by applying chemistry aspects, KSCE Journal of Civil Engineering 14(3) (2010) 333-341.

[5] K. Kanitpong, H.U. Bahia, Role of adhesion and thin film tackiness of asphalt binders in moisture damage of HMA, Association of Asphalt Paving Technologists Technical Sessions, 2003, Lexington, Kentucky, USA, 2003.

[6] A. Copeland, J. Youtcheff, N. Kringos, A. Scarpas, S. Mahadevan, Determination of bond strength as a function of moisture content at the aggregate-mastic interface, 10th International Conference on Asphalt Pavements-August 12 to 17, 2006, Quebec City, Canada, 2006.

[7] N. Ahmad, Asphalt mixture moisture sensitivity evaluation using surface energy parameters, University of Nottingham, 2011.

[8] R. Moraes, R. Velasquez, H. Bahia, Using bond strength and surface energy to estimate moisture resistance of asphalt-aggregate systems, Construction and Building Materials 130 (2017) 156-170.

[9] Z. Chen, S.-p. Wu, Z.-h. Zhu, J.-s. Liu, Experimental evaluation on high temperature rheological properties of various fiber modified asphalt binders, Journal of Central South University of Technology 15 (2008) 135-139.

[10] M. Mohammed, T. Parry, J. Grenfell, Fibre behaviour and influence on the properties of asphalt mortar, Bearing Capacity of Roads, Railways and Airfields (2017).

[11] J. Serfass, J. Samanos, Fiber-modified asphalt concrete characteristics, applications and behavior (with discussion), Journal of the Association of Asphalt Paving Technologists 65 (1996).

[12] H. Chen, Q. Xu, S. Chen, Z. Zhang, Evaluation and design of fiber-reinforced asphalt mixtures, Materials & Design 30(7) (2009) 2595-2603.

[13] A. Mahrez, M.R. Karim, H.Y.b. Katman, Fatigue and deformation properties of glass fiber reinforced bituminous mixes, Journal of the Eastern Asia Society for Transportation Studies 6 (2005) 997-1007.

[14] European Committee for Standardization, 1426: Bitumen and bituminous binders—determination of needle penetration, British Standards (2007).

[15] European Committee for Standardization, Bituminous mixtures - Test methods for hot mix asphalt - Part 18: Binder drainage, basket method, British Standard, 2004, pp. 5-10.

[16] British Standards, Part 143. Determination of asphaltenes (heptane insolubles) in crude petroleum and petroleum products, The institute of peteroleum and BSI 1996, London, 2000.

[17] D. ASTM, 4541, Standard Test Method for Pull-Off Strength of Coatings Using Portable Adhesion Testers, ASTM International: West Conshohocken, PA (2002).

[18] Mittal. K. L, Handbook of Adhesive Technology Second Edition, Revised and Expanded ed., Taylor & Francis Group, LLC, United States of America, 2003.

[19] D.N. Little, A. Bhasin, Using surface energy measurements to select materials for asphalt pavement, NCHRP Project 9-37, 2006.

[20] E.A. Masad, C. Zollinger, R. Bulut, D.N. Little, R.L. Lytton, Characterization of HMA moisture damage using surface energy and fracture properties (with discussion), Journal of the Association of Asphalt Paving Technologists 75 (2006).

[21] C. Van Oss, M. Chaudhury, R. Good, Monopolar surfaces, Advances in colloid and interface science 28 (1987) 35-64.

[22] P. Reynolds, T. Cosgrove, Colloid Science-Principles, Methods, and Applications, Blackwell Publishing Ltd, 2005.

[23] A. Bhasin, Development of methods to quantify bitumen-aggregate adhesion and loss of adhesion due to water, Texas A&M University, 2006.

[24] L. Oyekunle, Influence of chemical composition on the physical characteristics of paving asphalts, Petroleum Science and Technology 25(11) (2007) 1401-1414.

[25] F. Canestrari, F. Cardone, A. Graziani, F.A. Santagata, H.U. Bahia, Adhesive and cohesive properties of asphalt-aggregate systems subjected to moisture damage, Road Materials and Pavement Design 11(sup1) (2010) 11-32.

[26] B.J. Putman, Effects of fiber finish on the performance of asphalt binders and mastics, Advances in Civil Engineering 2011 (2011).

[27] J. Zhang, G.D. Airey, J.R. Grenfell, Experimental evaluation of cohesive and adhesive bond strength and fracture energy of bitumen-aggregate systems, Materials and Structures (2015) 1-15.

[28] R. Moraes, R. Velasquez, H. Bahia, Measuring the effect of moisture on asphalt-aggregate bond with the bitumen bond strength test, Transportation Research Record: Journal of the Transportation Research Board (2209) (2011) 70-81.

[29] S. Tapkın, A. Cevik, U. Usar, Prediction of Marshall test results for polypropylene modified dense bituminous mixtures using neural networks, Expert Systems with Applications 37(6) (2010) 4660-4670.

[30] H. Chen, Q. Xu, Experimental study of fibers in stabilizing and reinforcing asphalt binder, Fuel 89(7) (2010) 1616-1622.

[31] A.F. Faheem, H.U. Bahia, Modelling of asphalt mastic in terms of filler-bitumen interaction, Road Materials and Pavement Design 11(sup1) (2010) 281-303.

[32] R.G. Hicks, Moisture damage in asphalt concrete, Transportation Research Board1991.

[33] K.W. Kim, Y.S. Doh, S. Lim, Mode I reflection cracking resistance of strengthened asphalt concretes, Construction and Building Materials 13(5) (1999) 243-251.

[34] S. Tapkın, U. Usar, A. Tuncan, M. Tuncan, Repeated creep behavior of polypropylene fiber-reinforced bituminous mixtures, Journal of Transportation Engineering 135(4) (2009) 240-249.

[35] J.-S. Chen, K.-Y. Lin, Mechanism and behavior of bitumen strength reinforcement using fibers, Journal of Materials Science 40(1) (2005) 87-95.

[36] A.W. Hefer, Adhesion in bitumen-aggregate systems and quantification of the effect of water on the adhesive bond, Texas A&M University, 2005.